Multi-temporal analysis of submarine sand dunes morphodynamics (Bay of Brest, Brittany, France): A marker of sediment pathways in a macrotidal environment open to sea swells

Déborah Belleney, Axel Ehrhold, Nicolas Le Dantec, Pascal Le Roy, Gwenael Jouet

Multi-temporal analysis of submarine sand dunes morphodynamics (Bay of Brest, Brittany, France): a marker of sediment pathways in a macrotidal environment open to sea swells

Déborah Belleney[a*], Axel Ehrhold[b], Nicolas Le Dantec[c,d], Pascal Le Roy[c], Gwenael Jouet[b].

[a] Institut Universitaire Européen de la Mer, Geomer - UMR 6554 CNRS LETG, 29280 Plouzané, France
*deborah.belleney@univ-brest.fr
[b] IFREMER, Géosciences Marines, Centre de Brest, 29280 Plouzané, France
[c] Institut Universitaire Européen de la Mer, UMR 6538 Géosciences Océan, Technopôle Brest-Iroise, 29280, Plouzané, France
[d] Institut Universitaire Européen de la Mer, UMS 3113, Technopôle Brest-Iroise, 29280, Plouzané, France

ABSTRACT

Sediment structures including submarine banks and dune fields are ubiquitous on tide-dominated continental inner shelves such as in the Iroise Sea. These are of current interest to human activities in several respects: they constitute an obstacle to navigation, they are dredged for beach nourishment or exploited for marine aggregates. In addition, the morphodynamic characterising of these sedimentary structures improves the knowledge of the sediment transfers that occur in coastal areas. This study documents a submarine sand dune field located along the northern flank of the Goulet channel connecting the Bay of Brest to the Iroise Sea and the Bay of Biscay. Subject to a macrotidal regime with strong currents, and to large waves during storm events, this sedimentary system features large dunes with very high migration rates. The analysis of six bathymetric datasets (from March 2013 to October 2019) allows specifying the morphodynamic characteristics of this small dune field about 3.5 km in length and 500 m in width. These dunes have heights on the order of 0.5 m to 3.7 m with migration rates that can vary significantly within the range from 10 m/yr to 70 m/yr. The results highlight that the ebb tidal current and slope of the channel are the main factors controlling the evolution of these biogenic sandy structures migrating offshore (SW). Furthermore, seasonal variations in coastal hydrodynamics forcing, driven by tidal currents, appear to affect the temporal and spatial evolution of the dunes at this shorter time scale. This paper proposes a model of sediment transport patterns at the mouth of the bay of Brest according dune field characteristic, strong ebb current and residual tidal gyre.

ADDITIONAL INDEX WORDS: *sand body evolution, sediment transport, coastal sediment budget, hydro-geomorphological control*

1. INTRODUCTION

Characterising the dominant direction and pathways of sediment transport in inner continental shelf and coastal systems is essential for defining the extension of sedimentary cells and the long-term sedimentary budget of coastal systems. The defining character of these systems is that wave shoaling and breaking induce a mean landward-directed bottom shear stress and, therefore, mean sand movement towards the shore (Allen, 1968). Nevertheless, the littoral energy fence can be bypassed by large amounts of material during shoreface erosion by storm wave processes, river floods, and ebb tidal enhanced currents as observed for estuarine and tide-dominated coastal systems as addressed in this paper (Allen, 1968; Swift, 1976; Barnard *et al*., 2013; Fraccasia *et al*., 2016; Preston *et al*., 2018; Cruz and Noernberg, 2020). Overall, the assessment of sediment transfers, both cross-shore and longshore, between different components of the coastal system remains a major limitation in the understanding of the morphodynamics of nearshore and inner shelf sediment structures. This is partially due to the lack of high resolution datasets preventing full characterisation of coastal systems with seasonal variations of sedimentary fluxes (*e.g.* Ferret *et al*., 2010) but also recirculation pathways as described in numerous tidal coastal systems (Elias and Hansen, 2013 ; Fraccascia *et al*., 2016 ; Cruz and Noernberg, 2020). Nevertheless, sediment transport and sediment deposition, can be satisfactorily characterised by accurate monitoring of bedforms and other water-worked seabed features at the transition of shoreface and inner shelf. For instance, previous observations on submarine sand dunes have indicated a net seaward, regional scale, sediment transport in the San Francisco Bay coastal system, where tidal currents are enhanced by the inlet throat just inside Central Bay (Barnard *et al*., 2012a and 2013).

A similar approach is adopted in this paper focusing on the sediment transport and identification of controlling factors at the outlet of a large tide-dominated estuary system sheltered from the open sea by a narrow bedrock tidal inlet: the Bay of Brest located in the most western part of Brittany (France). The study is based on the observation of submarine dunes field at the outlet of the Bay of Brest in Western Brittany (France) where water flows reaches up to 50,000 m³/s during spring tide. The detailed examination of these submarine dunes and the characterisation of their migration is carried out on an original dataset of bathymetric surveys acquired over the last 7 years, with seasonal to annual intervals. It offers

opportunity to better understanding short time scales ranging from seasonal to multiannual processes controlling sediment transport at the mouth of a highly energetic inlet system with the specific questions about the factors controlling dune migration, while also explaining the resilience of the dune system over time.

2. STUDY AREA

2.1. Geographical, geological and sedimentary setting

The study area is located at the outlet of the Bay of Brest at the western extremity of the Brittany Peninsula and in the northern extremity of the Bay of Biscay (Figure 1.A). The Bay of Brest is a semi-closed basin of about 181 km², connected to the Iroise Sea by a relatively narrow channel ("The Goulet") about 1.8 km wide and 6 km long and oriented NE-SW (Fichaut, 1989; Ballèvre *et al*., 2009; Gregoire *et al*., 2016). To the north side of the outlet, the water depth ranges from -10 m (relative to Lowest Astronomical Tide, LAT) near the Minou Point to -57 m (LAT) at the bottom of a buried paleo-channel system (Gregoire *et al*., 2017).

This bay is characterised by three main sedimentary domains (Figure 1.B) (Gregoire *et al.*, 2016). First, the mud-prone estuarine domain in the upstream part of the bay (D1); mud is mixed in different proportions with other calcareous sediments. This upstream domain is fed by continental fluvial inputs. Second, the downstream part of the Bay (D2) characterised by mixed deposits composed of shelly, sandy gravel and pebbles. Finally, the sand-prone outlet of the Bay (D3) where the study area belongs. It is composed of sands (fine to gravelly) and shelly sands. This last domain exhibits a complex set of sedimentary features, including: i) a field of submarine sand dunes, this study focus, located on the right bank of the inlet at the outlet of the Bay of Brest (Figure 1.C. "Dune field: Study Area") (Gregoire *et al*., 2016). The granulometric signature of these dunes mainly consists of medium sand with high carbonate content (> 70% of total sediment weight); ii) another small dune field further west on the same bank of the channel. It is composed of 8 dunes which are between 0.5 m to 0.9 m high and their wavelength ranges from 24 m to 46 m (Figure 1.C. "Western dunes"). Their asymmetries are oriented from NE-SW; iii) a set of RSD (Ripple Scour Depression) located on the shallow platform extending northward of the D3 domain (the Bay of Bertheaume) (Figure 1.C. "RSD") (Gregoire *et al*., 2016); iiii) A comet marks field is also observed in the southern side of the channel, in Camaret Bay (Figure 1.C. "Comet marks"). The shape of these structures shown a dominate current oriented toward the NE due to sediment accumulation that occurred downstream of the obstruction.

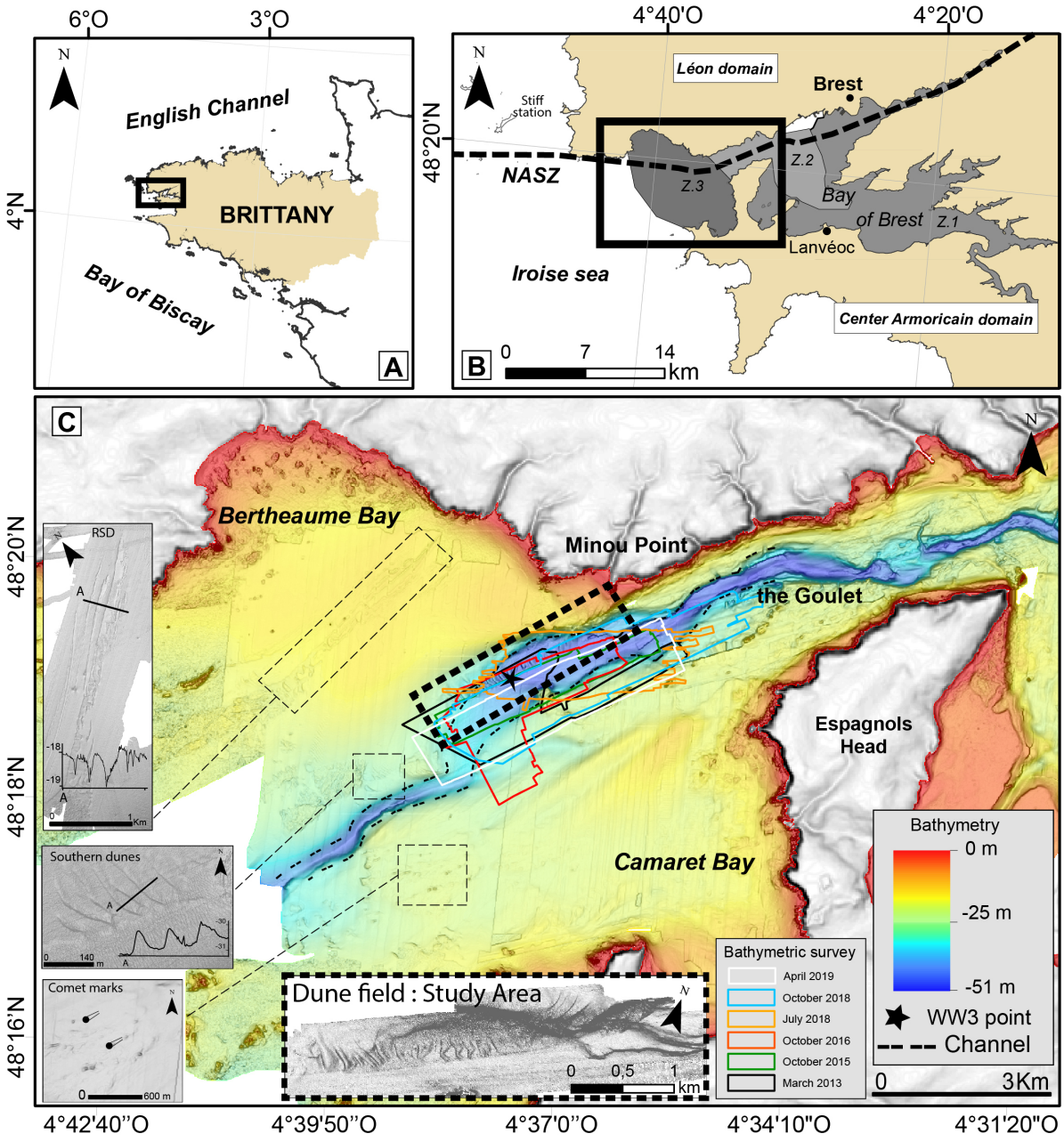

Figure 1: A) Location of the study area in western Brittany; B) Close-up view of the study area in the Bay of Brest and the Iroise Sea, D1: estuarine domain, D2: intermediate domain, D3: external domain (Gregoire *et al.*, 2016) (NASZ: North Armorican Shear Zone), Stiff station is a meteorological station; C) Detailed map with six successive bathymetric surveys (period 2013-2019) of the study area, and other sedimentary bedforms reported by Gregoire *et al.* (2016) (RSD: Ripple Scour Depression), the vertical scale of profiles is in meters, WW3 point is a wave statistics node from WaveWatch III® model.

2.2. Hydrodynamic setting

The tides are semi-diurnal with a tidal range varying from 1.22 m to 7.3 m. For spring tide, the flow current oriented ENE, can reach 2 m/s in the Goulet and decreases in the bay of Brest about 0.5 m/s. During the ebb period, the channel canalises the outflow and anticyclonic gyres are formed in the Camaret, and Bertheaume bays. Ebb current speeds can reach a maximum of 3.3 m/s at the Espagnols Head (SHOM, 1994). The analyses of MARS2D tide model from Previmer for spring-tide level (Figure 2.A and 2.B) show a maximum flow can reach 1.3 m/s during flood tide and 1.7 m/s during ebb tide in the Goulet. The tidal harmonic analysis from 2013 to 2019 (Figure 2.C. and Table 1) indicate a minimum of 0.33 m for 2015 and a maximum of 7.28 m for 2015 and 2019. The hours exceeded 6.65 m (mean high water spring) are 117 for 2016 and 2019 and 116 for 2015.

Data from WaveWatch III® model (Boudière *et al*., 2013) for the period 2010-2016, for a location in the Bay of Bertheaume over the studied dune field (-44 m depth; Figure 1.C for localisation of WW3 node) indicate a swell direction at 80% WSW and 20% SW. The significant wave heights range from 0. 25 m to 2 m 90% of the time, and from 2 m to 4 m 7% of the time. The same model indicates in storm conditions, for instance the 5 February 2014, a swell direction from WSW and 4-5 m height at the west extremity of dune field and 2-3 m height at the east extremity of dune field (Figure 2.D). During the last decade, several storms were recorded in Brittany (Table 2) by Météo-France (official service of meteorology and climatology in France). The 3 most morphogenetic storms have occurred during the 2013-2014 winter because they were combined with high spring tide levels (Blaise *et al*., 2015).

Table 1: Tidal range statistics from 2013 to 2014 in meters. The “occurrence > 6.65 m” indicate the number of hours that is exceeded for the mean high water spring level in Bertheaume Bay.

Year	Median	Min	Max	Occurrence > 6.65 m
2013	3.81	0.60	7.07	103
2014	3.82	0.41	7.23	111
2015	3.82	0.33	7.28	116
2016	3.81	0.39	7.16	117
2017	3.80	0.57	6.97	110
2018	3.80	0.51	7.18	100
2019	3.81	0.34	7.28	117

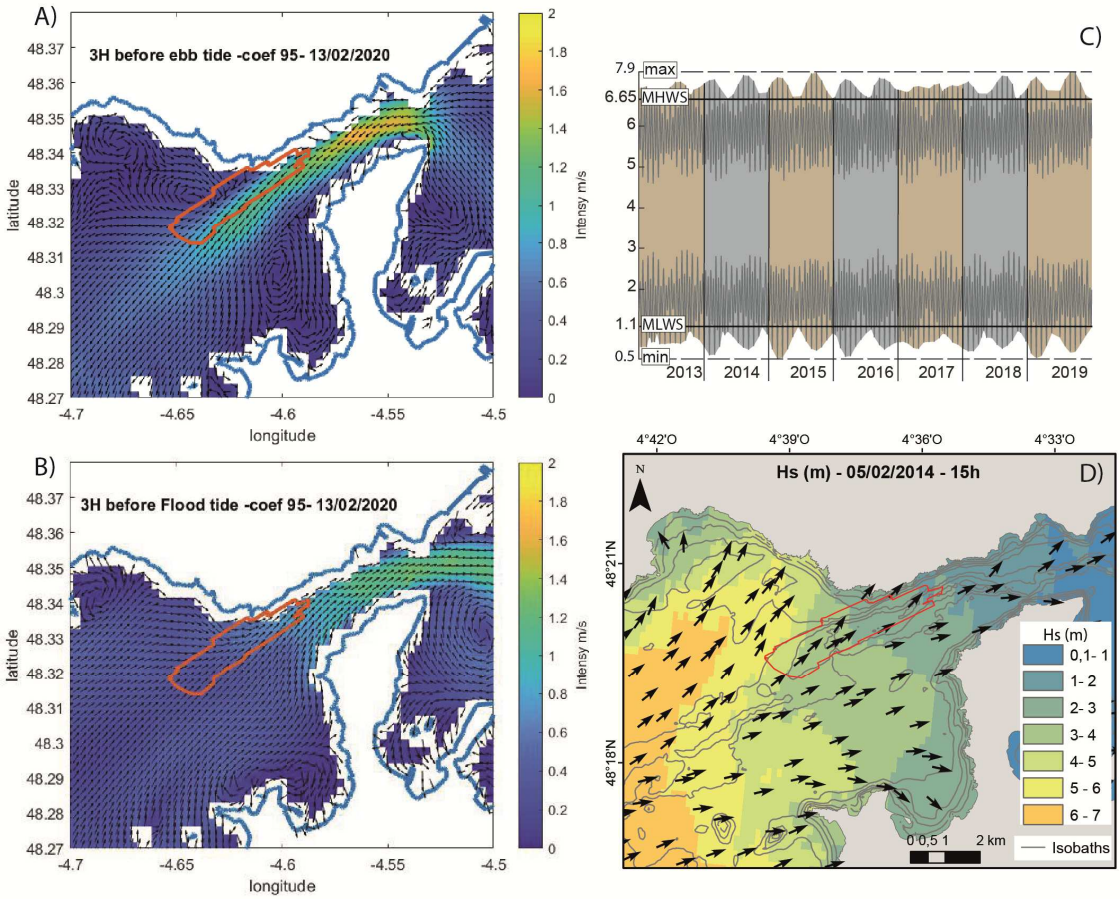

Figure 2: A) and B) tidal current during ebb and flood tide on 13 February 2020 from Previmer MARS2D tide model. C) The tidal harmonic from 2013 to 2019, the black lines represent the mean high water spring (MHWS) and the mean low water spring (MLWS), the dashed lines represent the maximum and minimum of the water level for the period 2013 to 2019 ; D) Wave height (Hs) and direction from WaveWatch III® model (5 February 2014).

Table 2: Historical storms registered in Brittany between 2013 and 2019 (data from Météo-France: www.meteofrance.com; Blaise *et al.*, 2015; Previmer: https://marc.ifremer.fr/ and Stiff Station: https://www.infoclimat.fr)

Storm	Day-Month	Year	Ouessant Stiff Station (Km/h)	Wind direction	Wave Hs (mean) Iroise sea (m)	Wave Hs direction
Dirk Noel	23-25 December	2013	>100	S	5.54	SW
Winter storms 2013-2014	1-4 January	2014	114	SSW	6.13	W
	1-3 February	2014	150	W	6.04	W
	2-3 March 2014	2014	114	NNW	6.75	W
Qendresa	3-4 November	2014	>100	SW	3.07	W
Zeus	6-7 March	2017	190	NW	3.49	W
Eleanor	3 January	2018	126	W	6.00	W

3. METHODS

3.1. Bathymetric Data

The analyses of dune morphology and sediment dynamics were done from bathymetric data acquired during six successive surveys realised by several institutions (Figure 1.C and Table 3). Bathymetric data were acquired using different multibeam echosounders (Table 3) with different GNSS (Global Navigation Satellite System) processing methods (Real Time Kinematic and Post Processed Kinematic). Data were processed using Qinsy-QPS software (IUEM data) and Globe software (IFREMER Data). The DTM of 2018 allowed to describe the morphology of the dunes with a resolution of 1 m. Dune migration was investigated at different time scales ranging from 4 and 6 months, 1 year, 2 years and 2.5 years, between March 2013 and April 2019.

Table 3: Configuration of survey acquisition systems (RTK: Real Time Kinematic*;* PPK: Post Processed Kinematic). DRASSM : Département des Recherches Archéologiques Subaquatiques et Sous-Marines; IFREMER : Institut Français de Recherche pour l'Exploitation de la MER ; IUEM/UBO : Institut Universitaire Européen de la Mer/Université de Bretagne Occidentale.

Survey Vessel	Institute	Date	acquisition system	DTM	vertical precision	horizontal precision	GPS treatment
Ess_dec_ata 19 Atalante	IFREMER	25-29/01/2019	Kongsberg EM710	1 m	1cm	1cm	RTK
Bertheaume Albert Lucas	IUEM/UBO	22-25/10/2018	Kongsberg EM3002	1 m	1cm	1cm	PPK
DRASSM André Malraux	DRASSM	02/07/2018	R2sonic 2024	1 m	1cm	1cm	PPK
Bertheaume Albert Lucas	IUEM/UBO	03-06/10/2016	Kongsberg EM3002	1 m	1cm	1cm	PPK
GeoLucas Albert Lucas	IUEM/UBO	27/10/2015	Kongsberg EM3002	1 m	1cm	1cm	PPK
Rebrade 2013 Thalia	IFREMER	03-07/03/2013	Kongsberg EM2040 D	2 m	1cm	1cm	RTK

3.2. Data Analysis

The morphodynamic dunes evolution results from the complex interaction between hydrodynamic conditions (tidal currents, swells, internal and storm waves), intrinsic sedimentary characteristics (lithology, grain size, amount of sediment available), and bedrock and sea level variations (Allen, 1968; Belderson *et al*., 1982; Berne *et al*., 1989 and 1993; Ashley, 1990; Idier *et al*., 2002; Le Bot and Trentesaux, 2004; Ferret *et al*., 2010). Therefore, it is essential to assess these morphological features by considering characteristic indexes

(height, wavelength, asymmetry…) to extract information about the surrounding environment (Allen, 1980; Langhorne, 1982; Berne *et al.*, 1989 and 1993; Beck *et al.*, 1991). For example, these measurements have been carried out on several dune fields in the Irish Sea to determine the dune growth mechanisms in relation to tidal energy (Van Landeghem *et al.*, 2009 and 2012).

The morphological kinematic of the dunes is performed from the mapping of crests. As developed in previous studies (*e.g.* Fraccascia *et al.*, 2016), the crest location is determined by the zero-crossing analysis and the residual migration between surveys was measured using a normal distance between crest displacements easy to identify from one year to another. The characteristics of the dunes were determined by DTM analysis using two specific software: 1) a GIS (geographic information system) software (ESRI™ ArcMap 10.6) to detect the crest of the dunes and to measure their migration, and 2) a spreadsheet program (Microsoft™ Excel 2016) to calculate, analyse and plot data, including morphometric characteristics such as the dune length or slope. Dune morphology was characterised using parameters and morphological indices commonly used by marine sedimentologists (Figure 3) (*e.g.* Allen, 1980; Langhorne, 1982; Berne *et al.*, 1989).

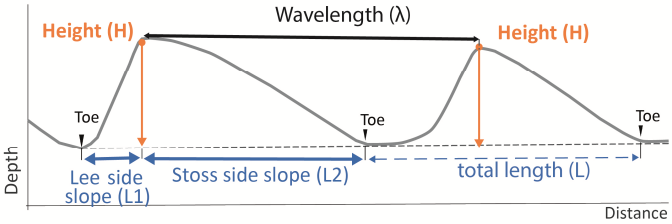

Figure 3: Morphological parameters of a transverse dune.

4. RESULTS

Bathymetric data revealed that dune field is composed of 30 submarine dunes extending southwestward over 3.5 km from the coastal headland Minou Point. Its lateral extension varies from 250 m to 400 m wide; It borders the northern part of the inlet and spreads from an upper terrace (the Bertheaume Terrace) from -10 m to -15 m to the deepest part of the inlet located at -50 m (Figure 4).

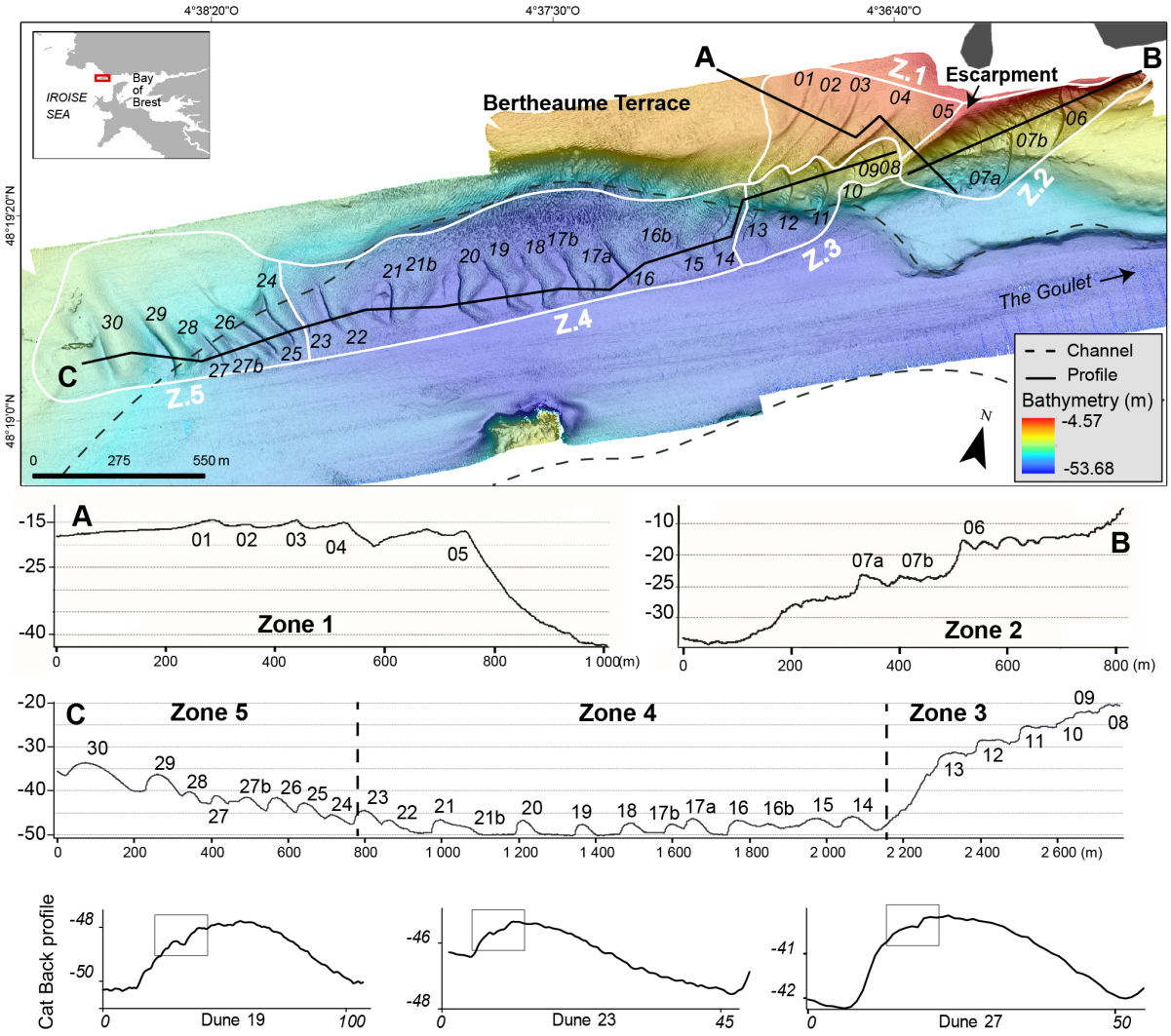

Figure 4: Detailed map of the studied dune field and dune crests defined using (dunes 1-30, grey lines) the October 2018 DTM with the cross-section profiles A, B, C and zones from Z.1 to Z.5 (Z. : zone). The profiles A, B, C illustrate the main morphological trends of the area. The profiles of dunes 19, 23 and 27 represent the cat-back shapes. The axes of the profiles are in meters.

4.1. Partitioning of dune field

Considering the heterogeneous morphology of the area, characterised by significant bathymetric variations ranging from -10 m to -50 m and the presence of the channel acting as valley guiding and enhancing tidal currents, the study area was segmented into according to characters of seafloor morphology: slopes, the water depth, location either on the terrace or channel. These 5 zones were established as follows (Figure 4). The Zone 1 is located at the northeast of the dune field, in the Bertheaume terrace, and includes dunes referenced 1 to 5, which exhibits an asymmetry oriented from NW to SE. Dune 5, located at the edge of the

terrace, connects zones 1 and 2. Dune 5 lies on a bathymetric step at - 25 m, between the top and the toe of the escarpment (slope up to 11°) corresponding to the northern edge of the channel. Zone 2 is located at the north-eastern end of the dune field and extends over the channel bank. It includes dunes 6 and 7 which exhibits an asymmetry oriented from NE to SW. These dunes are located on a steep slope of 8°. Zone 3 is located at the centre of the dune field along the toe of the channel bank. It includes dunes 8 to 13, which exhibits an asymmetry oriented from NE-SW. The average seafloor slope in zone 3 is 10°, inducing a 10 m variation of bathymetry over a length of 600 m. Zone 4 is located to the west of Zone 3, at a depth of about - 50 m corresponding to the deepest zone of the dune field and extends over a length of 1500 m. Extending along the talweg of the channel, it includes dunes 14 to 23 which exhibits an asymmetry oriented from NE-SW. Zone 5 is located in the western most part of the dune field and is characterized by southwestward decreasing depth along the channel bank and range from - 41 m to - 33 m (slope: 2.5 °). It includes dunes 24 to 30 which exhibits an asymmetry oriented from NE-SW.

4.2. Morphology of dunes

Morphological parameters are used to classify the dunes, determine their status (active or inactive) and evaluate their asymmetry (Allen, 1980; Knaapen, 2005). The morphological analysis of the dunes, based in October 2018 DTM, shows a high variability in their shape. The majority of dunes are between 0.5 m to 3.7 m high and their wavelength ranges from 10 m to 190 m long (Figure 5). More specifically, one third of the dunes are between 2 m and 2.5 m high, and half of them are between 60 m and 100 m long.

In this study, the angles of the lee side fluctuate between 5° and 30° with a median around 15.3 °. Regardless of the zones, a consistent pattern of lee slide slopes can be observed, which concerns 4 groups of 4 or 6 dunes forming successive sequences note S.A to S.D (Figure 5.A). These sets of dunes show gradual morphological changes, starting from a maximum angle and decreasing to a minimum value before reconstructing a new sequence. In each sequence, from east to west (direction of migration of the dunes), the significant slope values of the lee side (25°- 35°) decrease until about 10°. The sequences are identified as follows with the index of dunes: S.A: [6-10]; S.B: [11-16b]; S.C: [16-18]; S.D: [27-30].

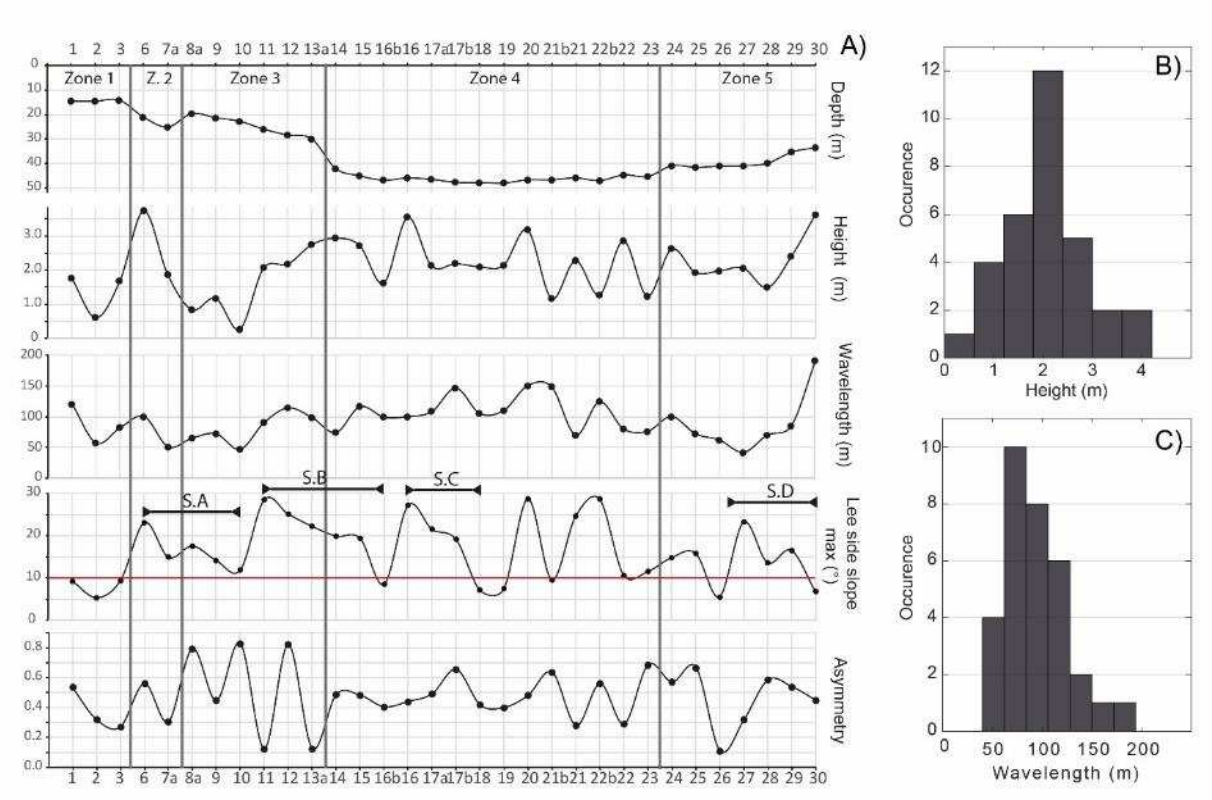

Figure 5: (A) Morphological characteristics (height, wavelength, lee side slope, and asymmetry) of the dunes 1 to 30, and water depth above the crest. The continuous lines are interpolations across the dune field along the profiles A to C. The red line on the plot shows the lee-side slope corresponds to a 10° slope, considered as the limit between inactive and active dunes (Belderson *et al*., 1982). The sequences S.A, S.B, S.C, and S.D describe a slope trend (lee side slope part). (B) and (C) Histograms of dune height and wavelength, respectively.

Dune asymmetry was calculated according to the formula of Knaapen (2005) [(L2-L1)/L] (Figure 3). For the dune field considered, asymmetry fluctuates between 0.1 and 0.8 (an average of 0.5) and shows a narrow range of variations between dunes 14 and 25, with asymmetry values contained within the range 0.3-0.7 (Figure 5.A). Dunes 6-8-10-12-17b-21b-23-25, have an asymmetry index above the maximum value of 0.6 measured by Van Landeghem *et al*. (2012) in the Irish Sea.

4.3. Height *vs* wavelength

In this study, the results obtained (Figure 5.A) show that height and wavelength seem to be well correlated in most parts of the field but presented in reality rapid fluctuations from one dune to another. The results, in terms of the distribution of heights and wavelengths of the

study area, are very similar to these of Flemming (2000) and Dalrymple (1984), but the coefficient of determination is rather small (R^2= 0.2) (Figure 6.A). Dunes within each zone seem to follow somewhat distinct correlation patterns (Table 4). In zones 1 and 3, with R^2 of 0.77 and 0.91 respectively, there is a good correlation between H and λ, noting that the exponent is higher than in the literature. Zone 2 is not evaluated for this rating because it comprises only two points. In zone 4, with the coefficient of 0.02, the correlation is very poor. In zone 5, the coefficient of determination (0.6) indicates an intermediate correlation between H and λ, with an exponent that remains lower than in the literature.

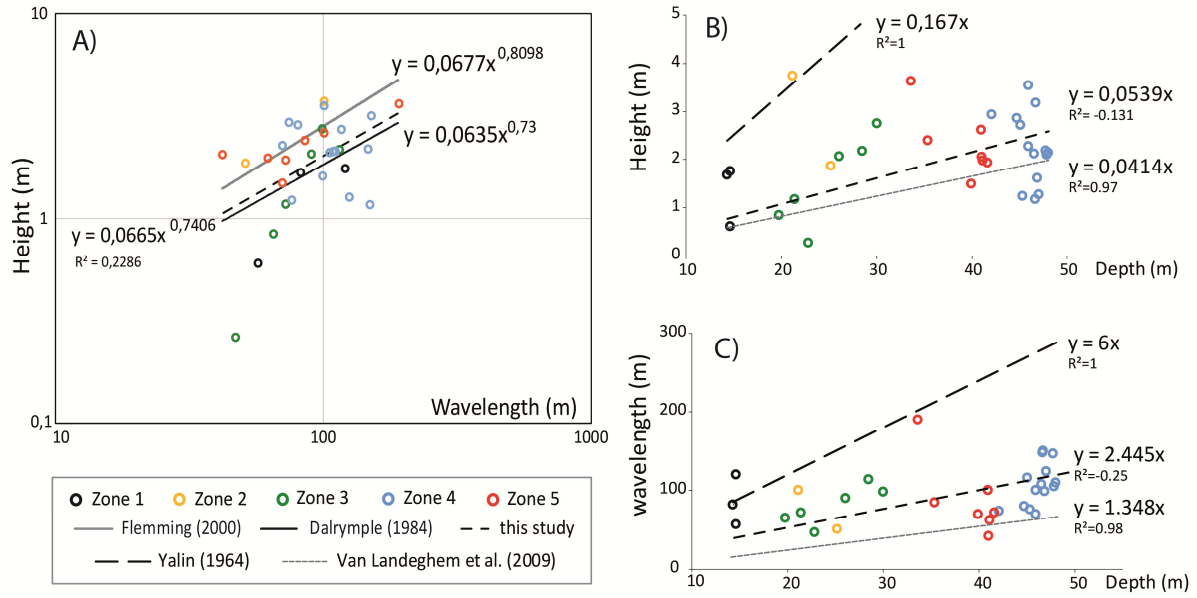

Figure 6: (A) Scatter plot of dune height *versus* wavelength with colours by zones of the dune field. Power law regressions and variance coefficients for each zone are summarised in Table 4. Power laws between dune dimensions and water depth compared with Van Landeghem *et al.* (2009) and Yalin (1964) observations; (B) Dune height *versus* water depth; (C) Dune wavelength *versus* water depth.

Table 4: Power law regressions of dune height *versus* wavelength (Figure 10) and coefficients of determination for zones 1 to 5.

Zone	Equation	R^2
1	$H= 0.0023*\lambda^{1.4247}$	0,77
2	$H= 0.0322*\lambda^{1.0322}$	1,00
3	$H= 0.00002*\lambda^{2.5864}$	0,91
4	$H= 5.1988*\lambda^{-0.194}$	0,02
5	$H= 0.2855*\lambda^{0.4674}$	0,60

4.4. Height or wavelength *vs* depth

Prior studies on other dune fields report an increase in dune height with increasing water depth (Yalin, 1964; Besio *et al*., 2006; Van Landeghem *et al*., 2009; Blondeaux and Vittori, 2011; Van Santen *et al*., 2011; Reynaud and Dalrymple, 2012). In this study, the relationship between dune height and water depth over the whole dune field is given by the power law $H = 0.0539*D$ (Figure 6.B), which is close to the equation obtained by Van Landeghem *et al*. (2009) in the Irish Sea, but with a very low $R^2 = 0.08$. The dune wavelength to water depth power law in this study corresponds to $\lambda = 2.445*D$ (Figure 6.C), which is also close to the equation obtained by Van Landeghem *et al*. (2009) in the Irish Sea. In zones 1 and 4, there is a range of dune height and wavelength whereas the depth remains nearly constant. In zone 3, where the bathymetry varies from -20 m to -30 m, there appears to be a good correlation between the increase in dune height and the increase in depth ($R^2 = 0.97$; dune 10 is excluded because it is less than 0.5 m high). A similar strong correlation appears between λ and depth in zone 5, where the dunes migrate upslope (from -41 m to -33 m); the regression analysis (with $R^2 = 0.54$) suggests decreasing dune height and wavelength with increasing water depth.

4.5. Dune migration

The dunes show different migration rates depending on the zone considered (Figure 7). At the scale of the dune field, there is an inverse relationship between migration rate and water depth. Dunes in zones 3 and 4 migrate very rapidly, around 60 m/yr, while dunes in zones 1, 2 and 5 migrate slower, around 20 m/yr. Considering these rates, it would take about 70 years for a dune initially positioned at the end of zone 3 to exit the system (end of zone 5). Considering each zone individually, the following trends can be noted. In zone 1, the rate decreases from dune 1 to dune 5 (from 37 m/yr to 10 m/yr, based on the July-October 2018 datasets). In zone 2, the only available data (October 2018 and April 2019) shows that the migration rate increases from dune 6 to dune 7 (from 18 m/yr to 24 m/yr). In zone 3, the speed of migration tends to increase lightly from 60 m/yr to 70 m/yr, except for dunes 9 and 10 considering the April 2019 dataset. From part of zone 3 and in most of zone 4, from dunes 11 to 20, the migration rate is relatively homogeneous, around 60-70 m/yr. From dune 21 to the western end of the dune field (rest of zone 4 and zone 5), the migration rate decreases to reach a low average value of around 10 m/yr. The migration rate is consistent

across all investigated time scales (4-6 months, 1-2-2.5 years), with a standard deviation varying from 1.3 m/yr to 12.7 m/yr (7.2 m/yr on average) over the whole area, and without outliers.

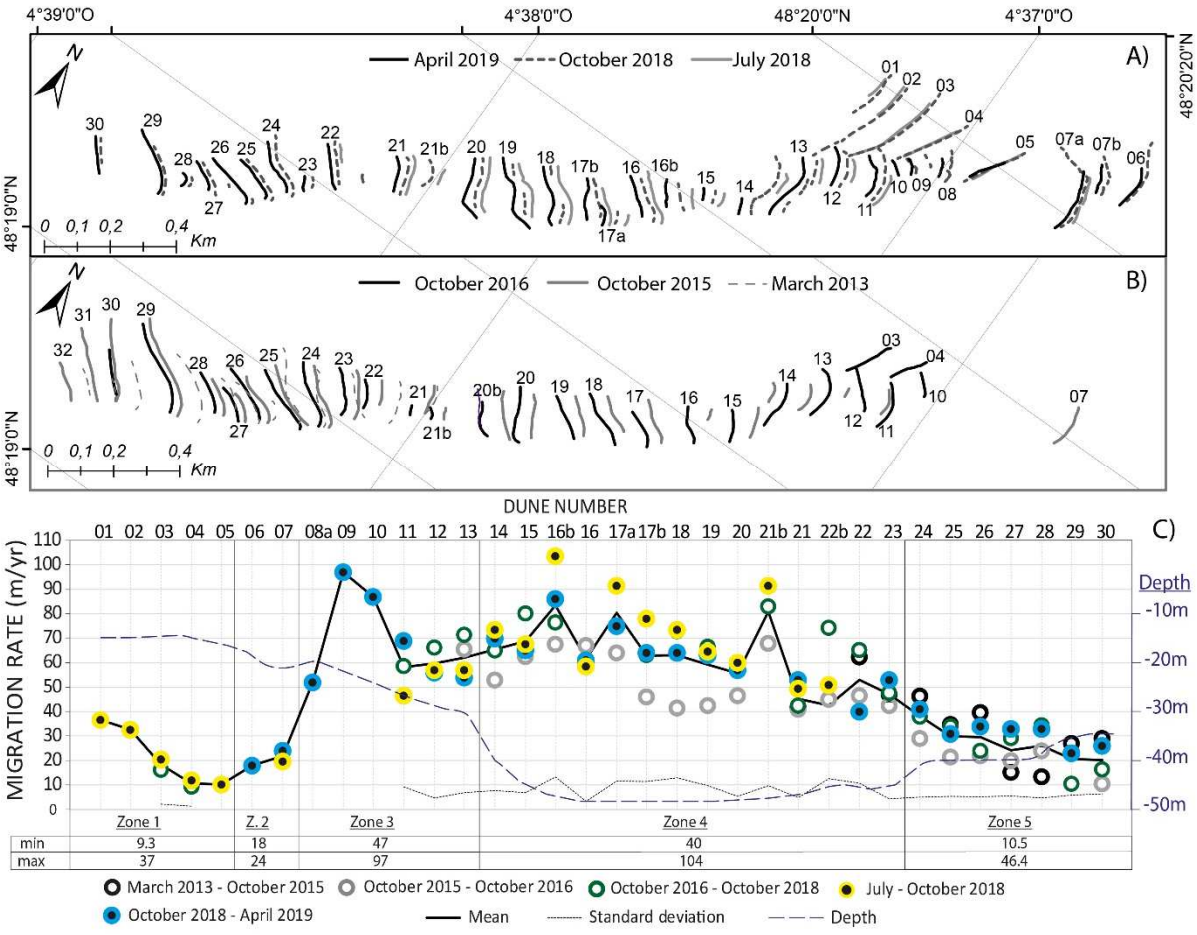

Figure 7: Migration of dune crests between (A) April 2019, October 2018 and July 2018 and (B) between March 2013, October 2015 and 2016; (C) Yearly migration rate according to the dune number (1 to 30) across the five zones. The black line represents the mean migration rate (m/yr) and the dotted line is the standard deviation per dune for different periods under consideration. The dashed line is the water depth.

The trends observed within each zone in a given year can also be seen in other years, except the high migration rate of dune 9 (97 m/yr) and 10 between October 2018 and April 2019, and the low migration rate of dunes 17b to 20 between October 2015 and 2016. The dataset allows examining seasonal effects on dune migration rates. Migration rates between

July and October 2018 correspond to the summer period (yellow symbol), while migration rates from October 2018 to April 2019 correspond to winter period (blue symbol). At this seasonal time scale, focusing on dunes 12 to 20 (zones 3 and 4), results suggest that the migration rate is systematically higher during the summer period (on the order of a few m by year). This seasonality in the migration rate is only noticeable in the central dune field (zones 3 and 4), which also corresponds to the deepest part of the dune field, in the channel bottom. Although here the migration rates are consistent across all investigated time scales, as was just noted, these results, derived from a summer to winter comparison over a single year, should be confirmed using a longer time series with bathymetric surveys acquired twice a year.

5. DISCUSSION

The morphodynamic characterisation of the dune field obtained through the interpretation of successive bathymetric DTMs shows that this nearshore submarine dune system changes over short distances, and is correlated with the seafloor morphology. The observed variability of forms and dynamics is analysed considering all the hydrodynamic and sedimentary factors.

5.1. Dune field morphology and equilibrium conditions

According to the classification of Berne *et al*. (1989), these sediment waves can be categorised as large to very large dunes. They are comparable to the dunes identified in other macrotidal coastal environments such as the Gironde estuary (Berne *et al*., 1993; Mallet *et al*., 2000) or Arcachon channel (Thauront *et al*., 1996), where dune heights vary between 1.6 m and 4.2 m and wavelengths between 58 m and 107 m. Submarine dunes with similar characteristics have also been observed in the shallow inner shelf (between -20 m to -40 m depth) and in the macrotidal context of the Pas de Calais Strait by Berne *et al*. (1989) and Le Bot and Trentesaux (2004). It is also the case for the Bay of San Francisco corresponding to another case of a highly energetic inlet system (Elias and Hansen, 2013) where dune size is similar to that of this present study at the same depth. Thus, dune size (height and wavelength), observed at the outlet of the Bay of Brest, is consistent with most of dune size case studies reported in examples of tidal coastal environments. Nevertheless, the "generally-accepted" correlation between dune height with wavelength and related power-laws (Allen, 1968; Dalrymple, 1978; Flemming, 2000; Francken et al., 2004) are not systematically applicable to the present case study. Thus, the analyses of the geometrical relationship

between λ and H, suggest that deeper (< -20 m) dunes (Z1 and Z2 areas) and those observed in steep slope (Z3 and Z5 areas) approach an equilibrium state. In contrast, the dunes located in the deepest part of the channel (Z4 area) where tidal currents are assumed to enhance by constriction of water flow are far from that equilibrium.

Prior studies on dune fields (*e.g*. Yalin, 1964) and recent works devoted to the process of the formation of tidal dunes have shown that predictions of the wavelengths of tidal dunes are strongly dependent on the mean water depth (Besio *et al*., 2006; Blondeaux and Vittori, 2011; Van Santen *et al*., 2011). Nevertheless, some authors indicate that correlation is not always clear (Dalrymple, 1978; Flemming, 1978; Ashley, 1990; Van Landeghem *et al*., 2009; Ferret *et al*., 2010) and suggest examining these predictions in relation to the studied coastal system. In this study, the good correlation between dune size and water depth, obtained in steep north flank of the channel (zones 3 and 5) suggests that a significant gradient in the bathymetry can play an important role in controlling dune growth. In contrast, zones 1 and 4 corresponding to a more planar seabed, show poor correlation between sizes of dunes and water depths. This result suggests that water depth is not a key control factor of dune grows on the planar area; it is probably more dependent on the variability of tidal currents in the deep and narrow inlet.

The morphology of the inlet is also involved in the control of lateral extension of dunes. Indeed, despite similar hydrodynamics settings, lateral extension of dunes is much greater in the mouth of San Francisco Bay where it reaches up to 1000 m (Elias and Hansen, 2013) than in the external domain of Bay of Brest (450 m). The main difference between these two mouths is the presence of a very marked paleochannel at the inlet of the Bay of Brest, in contrast to mouth of San Francisco Bay, where the bathymetry remains flatter. Thus, the presence of this well-marked incised valley limits the lateral extension of dunes.

In this study, the dunes generally show a very well-marked asymmetry (an average of 0.5), which is a signature of a single dominant current direction affecting dune morphology (Allen, 1980). However, in zones 4 and 5, most dunes have a cat-back profile, possibly indicative of a subordinate current in the opposite direction to the tidal residual current, and strong enough to reshape the top portion of the dune and smooth the dune crest.

5.2. Dunes migration

The measured migration rates show ample variations in space and time, with values ranging from 10 m/yr to 70 m/yr. According to the synthesis by Thauront *et al.* (1996),

submarine dune migration rates measured in this study are similar to those described in the literature (e.g. Langhorne, 1973 and 1982 and Berne *et al.*, 1989 b).

However, lee side slope patterns observed in October 2018, for several dunes (1, 2, 3, 16b, 18, 19) show values below 10° suggesting that the latter are not active (Belderson *et al.* 1982); however the migration rate records for these dunes are higher than 30 m/s between 2015 and 2019, show that the latter are mobile on a pluri-annual and seasonal scale. Moreover the apparent immobility of these dunes is difficult to be considered as stable over time in regard to the mobility of direct adjacent dunes. In consequence, the apparent inactivity of some dunes could rather be interpreted as a stationary state for a given period of time.

Changes in migration rates as a function of dune size, in zones 3 and 5, do not verify the classical inverse relationship, where migrating velocity is inversely proportional to the dune height and consequently to the dune size (e.g., Charru et al., 2013). This atypical behaviour can be discussed in the light of the morphology of the seafloor and associated hydrodynamics. In zone 3, the increase of migration rate is correlated with water depth. Similarly, in zone 5, the decrease of migration rate is observed to occur concomitantly with a decrease in water depth. For this latter zone, the seafloor slope is opposite to the migration direction, and expected to reduce the sediment transport rate. It is thus clear that the gradient of the seabed slope acts as a significant factor modulating the migration rate of dunes according to its orientation opposite to the same direction as dunes displacement. Moreover, the results also suggest that orientation of the bottom slope gradient has more influence on variations of migration rate than dune size. Thus, once the slope gradient of seabed is significant, the classical inverse relationship (height versus migration rate dunes) is not observed and the slope of the basal surface of dune migration controls the migration rate.

5.3. Control factors at different time scales

The tidal circulation appears to be the main factor controlling the direction of dune migration. Indeed the results show that the NE-SW migration direction of the dunes in channelised part (zones 2 to 5) is conformed to the ebb current orientation. At the opposite, out of the channelised part, the NW-SE current pattern along the Minou point is responsible for the direction of dune migration along the zone 1 whatever the flood or ebb periods. In this way, the dunes observed in the terrace (zone 1) are shaped by a residual current oblique to the main transport observed in the inlet. As shown by the current pattern (Figure 2.A), the dunes migration and sediment transport located to the north of the inlet are induced by a clockwise

gyre extending over the shallow Bertheaume Bay. Other studies of tidal channels show that these residual circulation gyres, positioned tips of the channel, are quite common and control the dune morphology that is maintained stable over time with a continuous recycled sand flux (Cruz and Noernberg, 2020 and Fraccasia *et al*., 2016).

From seasonal to annual scale, several authors noted that hydrodynamic agents such as tidal fluctuations and storms (waves and currents) can temporarily modify migration rates and even reverse migration directions (Grochowski *et al*., 1993; Van Dijk and Kleinhans, 2005; Le Bot *et al*., 2000 and 2006; Idier *et al*., 2002; Le Bot and Trentesaux, 2004; Ferret *et al*., 2010). Several hypotheses may explain variations in migration rates observed from one year to the next, with notably lower velocities between October 2015 and October 2016 (about 10 m/yr less than in other years). A first hypothesis is the effect of yearly variations in extreme tidal ranges and associated tidal currents. Larger would be the tide range, greater would be the shear stress on the seabed during ebb and flood. The comparison of tidal ranges over the period 2013-2018 shows that tidal ranges were largest in 2015-2016, implying higher transport capacity, associated tidal current velocities. This stronger bed shear stress of subordinate current (flood), occurred during the high string tide level, has a higher ability to slow down the progression of the dunes. Hence, variations of annual tidal range seem to have an impact on the annual rate of dune migration. Another hypothesis is that storm winds and high swells are able to remobilise sediments and reverse the direction of migration (Van Dijk and Kleinhans, 2005; Le Bot *et al*., 2000 and 2006; Idier *et al*., 2002; Le Bot and Trentesaux, 2004; Ferret *et al*., 2010). From 2015 to 2016, the French weather service (Météo-France) does not indicate any major storms. During the last decade, the most severe storms that impacted the Brittany coast, occurred during the winters of 2013-2014 and 2017. Unfortunately, the dataset lacks DTM in 2014 and 2017, which makes it unlikely to measure the direct effect of these storms on the morphodynamics of the dune field.

Over a tidal cycle, the macrotidal context of the Bay of Brest and the flow acceleration due to the narrow inlet is also susceptible to have a predominant role in the morphogenesis of the dunes. In this study, cat-back shapes were observed on some dunes located in the channel and may indicate the presence of subordinate currents opposite to the residual flow (McCave, 1971). Doré *et al*. (2017) showed that the flood current (here, the subordinate current) induces cat-back shapes on the morphology of tidal dunes in the Arcachon Channel. The same process occurs in the Bay of Brest, during spring flood, when the current velocity can reach 0.8 m/s, above the 0.5 m/s threshold necessary for dune initiation. At this study site, the reverse

current (flood) is further enhanced by the channelised context (-50 m water depth) and is strong enough to remobilise the sediment to the dune crest, thus providing cat-back shape.

5.4. Sediment transport patterns

Several sediment sources and sinks can be identified in the studied dune field. Material input occurs through the eastern and northeastern shallow end of the field and is controlled by the ebb and flood current. The exit of material occurs toward the southwestern deeper part of the channel (Figure 8). Overall, the migration of dunes indicates a steady-state net seaward sand transport at the outlet of the Brest Bay coastal system. The small western dune field, with an asymmetry oriented toward the SW confirm the net sediment transport toward the exit of the Bay of Brest and the Iroise Sea. Moreover, the tidal Bay of Bertheaume gyres, close to the channel and the field dune northwestern input (ISF in Figure 8), provide that a recirculation sediment loop can occur between this major dune field and the bay of Bertheaume and RSD. This indicated the presence of a little sediment cell in the middle of this embayment in connection with the northern flank of the tidal channel. In the southwestern part of the external domain relating to Camaret Bay, the outflow seems to be compensated by the flood current as suggested by the presence of comet marks oriented to the NE. However, the few sedimentary structures in this southern part suggest a more limited sediment transport.

What about other similar documented examples? The greatest similarity is with the mouth of San Francisco Bay, which is a similar macrotidal environment and almost identical mouth morphology due to the presence of an inlet channel opened onto two embayments on each side. According to Elias and Hansen (2012), the flow current (ebb and flood) at the exit of the San Francisco bay, produce residual tidal gyres in the embayments. Carefully, in San Francisco external domain, the recirculation eddy contribute to the beach stability. The same process occurs in the Bertheaume Bay where the ebb and flood gyres contribute to the recycling of sediment dunes. Thus, for both channel inlets subjected to reverse tidal currents, the recirculation eddy due to hydro-morphology context of these mouths (inlet channel opened into two embayments on each side), induce stability of sedimentary cells.

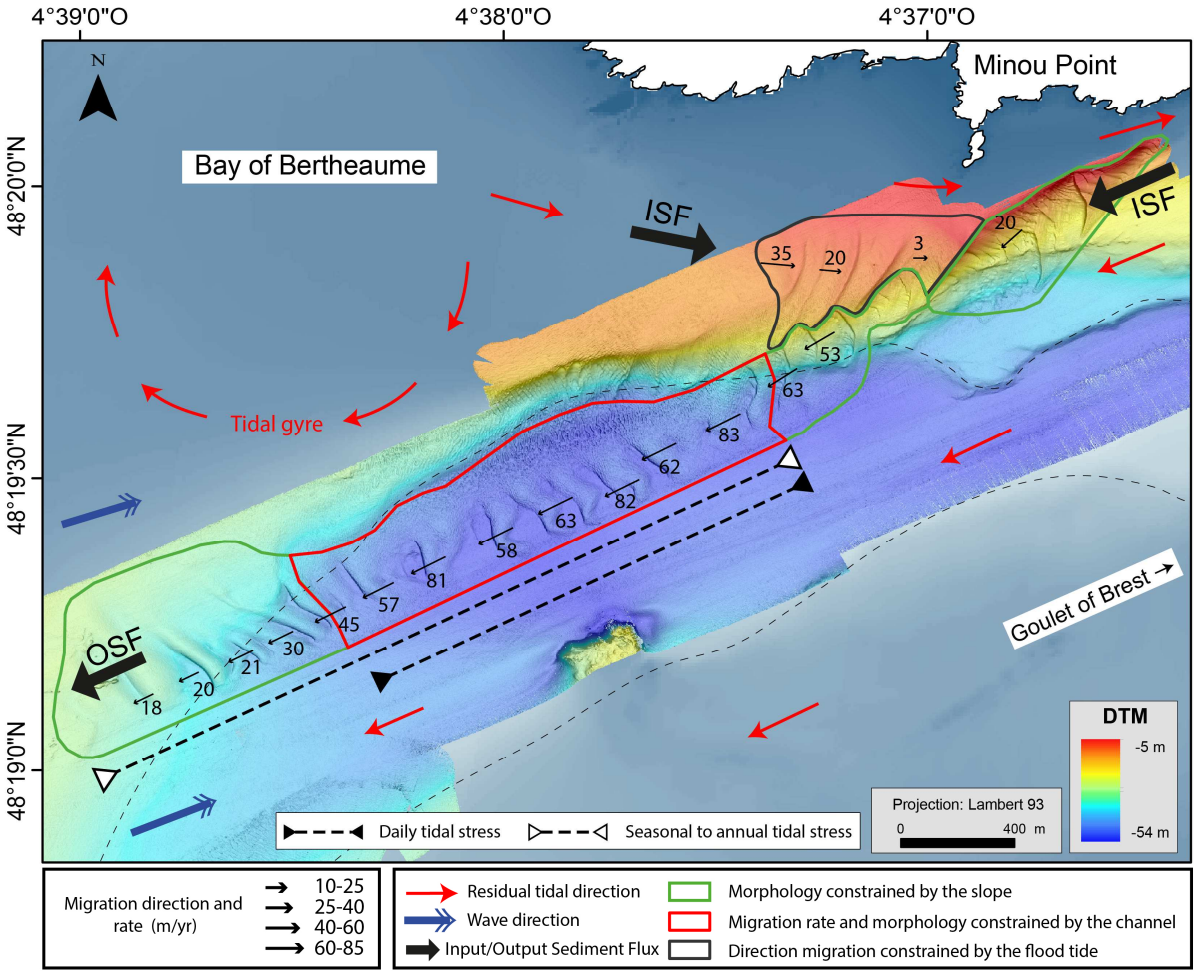

Figure 8: Conceptual diagram of dune field system in relation to residual tidal currents and waves. Areas where dune morphology is constrained by slope of seabed (green), the flood tide (black) and the ebb tide in the deep channel (red). The Sediment Flux Inputs (ISF) and Outputs (OSF) are also indicated.

6. CONCLUSIONS

This paper presents a submarine sand dunes morphodynamic monitoring at both the seasonal and pluriannual scales, which allows for defining the sediment transport pathway. The analysis of the dune morphology and migration rate has highlighted several characteristics as follows:

The sizes of the dunes, observed at the outlet of the Bay of Brest, is consistent with previous studies related to tidal coastal environments. However, the equilibrium of the dunes is only obtained in the deepest zones, above -30 m and in steep slopes area. This narrow inlet channel, exposed to the tidal current, prevents the usual development of the dunes below depth of 15 m. Water depth is not a significant control factor for dunes growth which is more dependent on the disparity of tidal currents through the deep and narrow channel.

In this macrotidal context, the ebb current appears the main factor that control the rate and direction of dunes migration. The flood current could be the origin of a decrease in the migration rate during higher tidal range periods, due to an increase in the shear stresses on the seabed in the opposite direction of migration. The second factor controlling morphology and migration rate is the seabed morphology specifically the strongly incised channel and these steep slopes. Indeed, the slope gradient of the seabed also acts as a significant factor modulating the migration rate and limiting the lateral extension of dunes.

Finally, the morphodynamic analysis of this dune field has revealed that the sediment transfers at the Bay of Brest mouth are mainly oriented toward the Iroise Sea. However, a circular sediment cell has been identified between the embayment and the inlet channel in relation to the tidal gyres. Thus, part of the sedimentary material supplying the dune field would be recycled by this tidal gyre. Subsequently, it would be interesting to carry out sediment transport modelling to improve these results. The study of dune morphodynamics has therefore allowed us to improve our knowledge of sediment transport, an essential key to understanding the management of marine human activities.

Declaration of competing interest

The authors declare that they have no known competing financial interests or personal relationships that could have appeared to influence the work reported in this paper.

Acknowledgments

The authors would like to thank the crew of Research Vessel Albert Lucas, Marcaurélio Franzetti, Mickaël Beauverger and Christophe Prunier (LGO engineers) for their contribution to data collection, the "Département des recherches archéologiques subaquatiques et sous-marines (DRASSM)" for providing us with the bathymetric dataset of July 2018, Hervé Bisquay (Hydrographer in charge of data quality at Genavir) for providing us bathymetric with the dataset of April 2019, and Stephane Bertin for his careful proofreading.

References

Allen, J.R.L., 1968. The Nature and Origin of Bed-Form Hierarchies. Sedimentology 10, 161–182. https://doi.org/10.1111/j.1365-3091.1968.tb01110.x

Allen, J.R.L., 1980. Sand waves: A model of origin and internal structure. Sedimentary Geology 26, 281–328. https://doi.org/10.1016/0037-0738(80)90022-6

542 Ashley, G.M., 1990. Classification of large-scale subaqueous bedforms; a new look at an old
543 problem. Journal of Sedimentary Research 60, 160–172. https://doi.org/10.2110/jsr.60.160
544 Ballèvre, M., Bosse, V., Ducassou, C., Pitra, P., 2009. Palaeozoic history of the Armorican
545 Massif: Models for the tectonic evolution of the suture zones. Comptes Rendus Geoscience
546 341, 174–201. https://doi.org/10.1016/j.crte.2008.11.009
547 Barnard, P.L., Erikson, L.H., Rubin, D.M., Dartnell, P., Kvitek, R.G., 2012a. Analyzing
548 bedforms mapped using multibeam sonar to determine regional bedload sediment transport
549 patterns in the San Francisco Bay coastal system. In: Li, M.Z., Sherwood, C.R., Hill, P.R.
550 (Eds.), Sediments, Morphology and Sedimentary Processes on Continental Shelves:
551 Advances in Technologies, Research and Applications: International Association of
552 Sedimentologists (IAS) Special Publication 44, pp. 272–294.
553 Barnard, P.L., Schoellhamer, D.H., Jaffe, B.E., McKee, L.J., 2013. Sediment transport in the
554 San Francisco Bay Coastal System: An overview. Marine Geology 345, 3–17.
555 https://doi.org/10.1016/j.margeo.2013.04.005
556 Beck, C., Clabaut, P., Dewez, S., Vicaire, O., Chamley, H., Augris, C., Hoslin, R., Caillot, A.,
557 1991. Sand bodies and sand transport paths at the English Channel-North Sea border:
558 Morphology, dynamics and radioactive tracing. Oceanologica Acta 11, 111–121.
559 Belderson, R.H., Johnson, M.A. and Kenyon, N.H., 1982. Offshore tidal sand. In: Stride, A.H.
560 (Eds.), Processes and deposits. Chapman and Hall Ltd, London, pp. 27-57.
561 Berne, S., Allen, G., Auffret, J.P., Chamley, H., Durand, J., Weber, O., 1989. Essai de
562 synthese sur les dunes hydrauliques geantes tidales actuelles. Bulletin de la Société
563 Géologique de France V, 1145–1160. https://doi.org/10.2113/gssgfbull.V.6.1145
564 Berne, S., Castaing, P., Drezen, E.L., Lericolais, G., 1993. Morphology, internal structure,
565 and reversal of asymmetry of large subtidal dunes in the entrance to Gironde Estuary
566 (France). Journal of Sedimentary Research 63, 780–793.
567 https://doi.org/10.1306/D4267C03-2B26-11D7-8648000102C1865D
568 Besio, G., Blondeaux, P., Vittori, G., 2006. On the formation of sand waves and sand banks.
569 Journal of Fluid Mechanics 557, 1–27. https://doi.org/10.1017/S0022112006009256
570 Blaise, E., Suanez, S., Stéphan, P., Fichaut, B., David, L., Cuq, V., Autret, R., Houron, J.,
571 Rouan, M., Floc'h, F., Ardhuin, F., Cancouët, R., Davidson, R., Costa, S., Delacourt, C.,
572 2015. Bilan des tempêtes de l'hiver 2013-2014 sur la dynamique de recul du trait de côte
573 en Bretagne. Géomorphologie : relief, processus, environnement 21, 267–292.
574 https://doi.org/10.4000/geomorphologie.11104

575 Blondeaux, P., Vittori, G., 2011. The formation of tidal sand waves: Fully three-dimensional
576 versus shallow water approaches. Continental Shelf Research 31, 990–996.
577 https://doi.org/10.1016/j.csr.2011.03.005
578 Boudière, E., Maisondieu, C., Ardhuin, F., Accensi, M., Pineau-Guillou, L., Lepesqueur, J.,
579 2013. A suitable metocean hindcast database for the design of Marine energy converters.
580 International Journal of Marine Energy 3, e40–e52.
581 https://doi.org/10.1016/j.ijome.2013.11.010
582 Charru, F., Andreotti, B., Claudin, P., 2013. Sand Ripples and Dunes. Annual Review of
583 Fluid Mechanics 45, 469–493. https://doi.org/10.1146/annurev-fluid-011212-140806
584 Cruz, O.G., Noernberg, A.M., 2020. Bedforms controlled by residual current vortices in a
585 subtropical estuarine tidal channel. Estuarine, Coastal and Shelf Science 232, 106485.
586 https://doi.org/10.1016/j.ecss.2019.106485
587 Dalrymple, R.A., 1978. Rip currents and their causes. Coastal Engineering 1978: Proceedings
588 of the 16th International Conference. Am. Soc. Civ. Eng, New York, pp.1414–1427.
589 Dalrymple, R.W., 1984. Morphology and internal structure of sandwaves in the Bay of
590 Fundy. Sedimentology 31, 365–382. https://doi.org/10.1111/j.1365-3091.1984.tb00865.x
591 Doré, A., Bonneton, P., Marieu, V., Garlan, T., 2017. Observation and numerical modeling of
592 tidal sand dune dynamics. Coastal Dynamics 90, 17–21
593 Ehrhold, A., Le Gall, B., Stéphan, P., Suanez, S.S., 2017. Présentation générale. In: Ehrhold,
594 A., B.L.G. (Ed.), Atlas de l'archipel de Molène. Géologie, Géomorphologie et
595 Sédimentologie. Quae, Versailles, pp. 17–32.
596 Elias, E.P.L., Hansen, J.E., 2013. Understanding processes controlling sediment transports at
597 the mouth of a highly energetic inlet system (San Francisco Bay, CA). Marine Geology
598 345, 207–220. https://doi.org/10.1016/j.margeo.2012.07.003
599 Ferret, Y., Bot, S.L., Tessier, B., Garlan, T., Lafite, R., 2010. Migration and internal
600 architecture of marine dunes in the eastern English Channel over 14 and 56 year intervals:
601 the influence of tides and decennial storms. Earth Surface Processes and Landforms 35,
602 1480–1493. https://doi.org/10.1002/esp.2051
603 Ferret, Y., Bot, S.L., Tessier, B., Garlan, T., Lafite, R., 2010. Migration and internal
604 architecture of marine dunes in the eastern English Channel over 14 and 56 year intervals:
605 the influence of tides and decennial storms. Earth Surface Processes and Landforms 35,
606 1480–1493. https://doi.org/10.1002/esp.2051

607 Flemming, B.W., 1978. Underwater sand dunes along the southeast African continental
608 margin Observations and implications. Marine Geology 26, 177–198.
609 https://doi.org/10.1016/0025-3227(78)90059-2
610 Fraccascia, S., Winter, C., Ernstsen, V.B., Hebbeln, D., 2016. Residual currents and bedform
611 migration in a natural tidal inlet (Knudedyb, Danish Wadden Sea). Geomorphology 271,
612 74–83. https://doi.org/10.1016/j.geomorph.2016.07.017
613 Francken, F., Wartel, S., Parker, R., Taverniers, E., 2004. Factors influencing subaqueous
614 dunes in the Scheldt Estuary. Geo-Marine Letters 24, 14–21.
615 https://doi.org/10.1007/s00367-003-0154-x
616 Gregoire, G., 2016. Dynamique sédimentaire et évolution holocène d'un système macrotidal
617 semi-fermé : l'exemple de la rade de Brest. Ph.D. Thesis. Université de Bretagne
618 occidentale, Brest.
619 Gregoire, G., Ehrhold, A., Roy, P.L., Jouet, G., Garlan, T., 2016. Modern morpho-
620 sedimentological patterns in a tide-dominated estuary system: the Bay of Brest (west
621 Britanny, France). Journal of Maps 12, 1152–1159.
622 https://doi.org/10.1080/17445647.2016.1139514
623 Gregoire, G., Le Roy, P., Ehrhold, A., Jouet, G., Garlan, T., 2017. Control factors of
624 Holocene sedimentary infilling in a semi-closed tidal estuarine-like system: the bay of
625 Brest (France). Marine Geology 385, 84–100.
626 https://doi.org/10.1016/j.margeo.2016.11.005
627 Grochowski, N., Collins, M., Boxall, S., Salomon, J., Breton, M., Lafite, R., 1993. Sediment
628 transport pathways in the eastern english-channel. Oceanologica Acta 16, 531–537.
629 Hallegouet, B., Lozac'h, G., Vigouroux, F.,1994. Formation de la rade de Brest. In : Corlaix,
630 J.P. (Eds.), Atlas permanent du littoral. Editmar, France, p. 22.
631 Idier, D., Ehrhold, A., Garlan, T., 2002. Morphodynamique d'une dune sous-marine du détroit
632 du pas de Calais. Comptes Rendus Geoscience 334, 1079–1085.
633 Knaapen, M. a. F., 2005. Sandwave migration predictor based on shape information. Journal
634 of Geophysical Research: Earth Surface 110, F4. https://doi.org/10.1029/2004JF000195
635 Langhorne, D.N., 1973. A sandwave field in the Outer Thames Estuary, Great Britain. Marine
636 Geology 14, 129–143. https://doi.org/10.1016/0025-3227(73)90056-X
637 Le Bot, S., Trentesaux, A., Garlan, T., Berne, S., Chamley, H., 2000. Influence des tempêtes
638 sur la mobilité des dunes tidales dans le détroit du Pas-de-Calais. Oceanologica Acta 23,
639 129–141. https://doi.org/10.1016/S0399-1784(00)00115-8

Le Bot, S., Trentesaux, A., 2004. Types of internal structure and external morphology of submarine dunes under the influence of tide- and wind-driven processes (Dover Strait, northern France). Marine Geology 211, 143–168. https://doi.org/10.1016/j.margeo.2004.07.002

Ma, X., Yan, J., Fan, F., 2014. Morphology of submarine barchans and sediment transport in barchans fields off the Dongfang coast in Beibu Gulf. Geomorphology 213, 213–224. https://doi.org/10.1016/j.geomorph.2014.01.010

Mallet, C., Howa, H.L., Garlan, T., Sottolichio, A., Hir, P.L., 2000. Residual Transport Model in Correlation with Sedimentary Dynamics over an Elongate Tidal Sandbar in the Gironde Estuary (Southwestern France). Journal of Sedimentary Research 70, 1005–1016. https://doi.org/10.1306/022900701005

McCave, I.N., 1971. Sand waves in the North sea off the coast of Holland. Marine Geology 10, 199–225

Preston, J., Hurst, M.D., Mudd, S.M., Goodwin, G.C.H., Newton, A.J., Dugmore, A.J., 2018. Sediment accumulation in embayments controlled by bathymetric slope and wave energy: Implications for beach formation and persistence. Earth Surface Processes and Landforms 43, 2421–2434. https://doi.org/10.1002/esp.4405

Reynaud, J.-Y., Dalrymple, R.W., 2012. Shallow-Marine Tidal Deposits, in: Davis, R.A., Dalrymple, R.W. (Eds.), Principles of Tidal Sedimentology. Springer Netherlands, Dordrecht, pp. 335–369. https://doi.org/10.1007/978-94-007-0123-6_13

Service Hydrographique et Océanographique de la Marine, SHOM. (1994). Atlas des courants de marée : Courants de marée de la côte Ouest de Bretagne. S.H.O.M, France.

Swift, D. J., 1976. Coastal sedimentation. In: Stanley, D.J. and Swift, D.J.P (Eds.), Marine Sediment Transport and Environmental Management, Wiley, New York, pp. 255-309.

Thauront, F., Berne, S. and Cirac, P., 1996. Tidal dune morphology and seasonal changes in the bay of Arcachon, France. Comptes Rendus de l'Académie des Sciences de Paris (II a), 323, pp. 411-418.

Todd, B.J., 2005. Morphology and composition of submarine barchan dunes on the Scotian Shelf, Canadian Atlantic margin. Geomorphology 67, 487–500. https://doi.org/10.1016/j.geomorph.2004.11.016

Van Dijk, T.A.G.P., Kleinhans, M.G., 2005. Processes controlling the dynamics of compound sand waves in the North Sea, Netherlands. Journal of Geophysical Research: Earth Surface 110, Issue F4. https://doi.org/10.1029/2004JF000173

673 Van Landeghem, K.J.J., Wheeler, A.J., Mitchell, N.C., Sutton, G., 2009. Variations in
674 sediment wave dimensions across the tidally dominated Irish Sea, NW Europe. Marine
675 Geology 263, 108–119. https://doi.org/10.1016/j.margeo.2009.04.003
676 Van Landeghem, K.J.J., Baas, J.H., Mitchell, N.C., Wilcockson, D., Wheeler, A.J., 2012.
677 Reversed sediment wave migration in the Irish Sea, NW Europe: A reappraisal of the
678 validity of geometry-based predictive modelling and assumptions. Marine Geology 295,
679 95–112. https://doi.org/10.1016/j.margeo.2011.12.004
680 Van Santen, R.B., de Swart, H.E., van Dijk, T.A.G.P., 2011. Sensitivity of tidal sand
681 wavelength to environmental parameters: A combined data analysis and modelling
682 approach. Continental Shelf Research 31, 966–978.
683 https://doi.org/10.1016/j.csr.2011.03.003
684 Yalin, M.S., 1964. Geometrical Properties of Sand Wave. Journal of the Hydraulics Division
685 90, 105–119.
686
687